

Nanocomposites by rapid solidification route

K CHATTOPADHYAY

Department of Metallurgy, Indian Institute of Science, Bangalore 560 012, India

Abstract. Nanometric aggregates of solids can be classified into two types, nanograined or nanophased materials and nanocomposites. In the present paper after a brief review including the relation between size and boundary fraction, the basic principles that can be utilized to synthesize these materials from liquid route has been discussed. We shall present examples to show that with proper choice of systems and conditions it is possible to obtain nanocomposites in systems showing clustering tendencies in liquid as well as the systems exhibiting ordering tendencies leading to compound formation.

Keywords. Nanocomposites; rapid solidification route.

1. Introduction

The scale of microstructure plays an important role in controlling the properties of materials. Metallurgical literature abounds with efforts to refine the scale of microstructure to improve properties. The classical examples include the strengthening by grain boundaries following Hall-Petch relationship and improving chemical homogeneity by chill casting. Although the grain and interface boundaries often play important roles in controlling the properties of conventional materials, the volume fraction occupied by these boundaries rarely exceeds a few percent. The influence is indirect and the properties of the boundaries do not influence any bulk properties. With the recent development of nanostructural materials the possibility of the grain and interface boundaries contributing significantly to the overall bulk properties becomes a reality (Gleiter 1989).

We now attempt to provide a definition of nanostructural material. In general a material qualifies to be called a nanoscaled material, if the volume fraction of the grain or interphase boundary is of the order of 30% of the total volume. However, it is important to point out that there cannot be any rigid quantification. The basic qualification is to have grain/interphase boundary component significant enough to have an impact on the overall properties under consideration. It is clear, therefore, that the volume fraction requirement depends upon the nature of the property under consideration. For example, large volume fraction of boundary component is necessary for bulk properties like excess volume or specific heat. On the other hand the boundaries effect may be felt at much lower volume fraction for certain class of mechanical and electrical properties.

In two-phase materials, nanoscale structures can be of two types. In one both the phases may exist in very fine scale. On the other hand an ultrafine dispersion of the second phase in the primary matrix also can produce a large amount of interphase interface which is capable of influencing the properties. The latter class of materials is also referred to as nanocomposites. It is pertinent to emphasize that there exists large varieties of materials which are in nanoscale without aggregation. These particles, generally known as clusters, can exhibit very novel properties (Jena *et al* 1989). However, these are excluded from the present discussion where we shall deal

exclusively with the aggregated solids composed of nanoscale grains/phases and nanocomposites.

2. Relationship between size and volume fraction in nanomaterials

It is possible to have a simple estimate of the boundary fraction from geometrical consideration. We assume that all the grains have identical shape and uniform size. Further, nanomaterials are produced by fragmenting a single crystal of volume v_0 . The corresponding initial surface and radius are S_0 and r_0 respectively. The number of grains (n) generated after fragmentation to a radius r_1 is given by the following equation

$$n = r_0^3/r_1^3 \quad (1)$$

Total grain boundary area S_1 created in the process is

$$S_1 = \left(\frac{r_0}{r_1}\right) S_0 \quad (2)$$

Assuming T as the thickness of the boundary, the volume fraction of the boundary regions V_b^f is given by

$$v_b^f = \frac{V_b}{V_0} = A(T/r_1) \quad (3)$$

Here A is a constant which depends on the shape factor and is 3 for spherical approximation (Mütschele and Kirchheim 1987). If the boundary thickness is of the order of 1 nm the above expression indicates that for 0.3 volume fraction of boundary regions, the particles need to have a radius of 10 nm. Figure 1 shows a plot of boundary volume fraction as a function of particle size for spherical approximation.

We now consider the case when second phase particles are dispersed in nanoscale in a coarse grained matrix. For this case

$$V_p + V_m = 1 \quad (4)$$

where V_p and V_m are the volume fractions of the particles and matrix respectively. Let the thickness of the interphase boundary regions be T and assuming that the boundaries are entirely confined in the matrix volume and neglecting volume change due to a possible change of density we obtain the boundary fraction as given below

$$V_b^f = V_p^f \frac{A \cdot T}{r_1} \quad (5)$$

where A , a constant, which depends on geometrical factor. Again assuming T of the order of 1 nm, figure 2 gives the relation between dispersion size (radius r_1) and boundary volume fraction V_b^f for different volume fractions of dispersed phase V_p^f assuming spherical dispersoids. The above estimates indicate significant boundary volume fraction when the scale of microstructure is in nanometer regime both for nanocrystalline materials and nanocomposites.

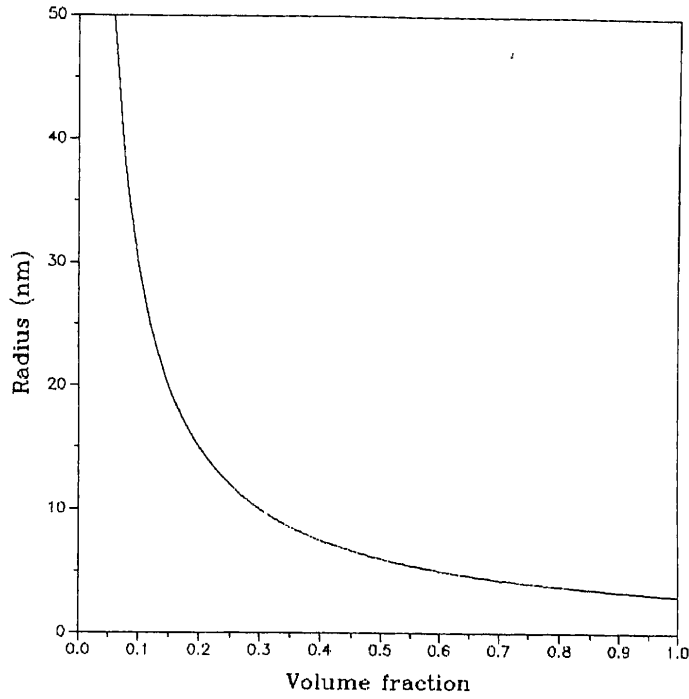


Figure 1. A plot showing the relation between boundary volume fraction as a function of particle size for spherical approximation.

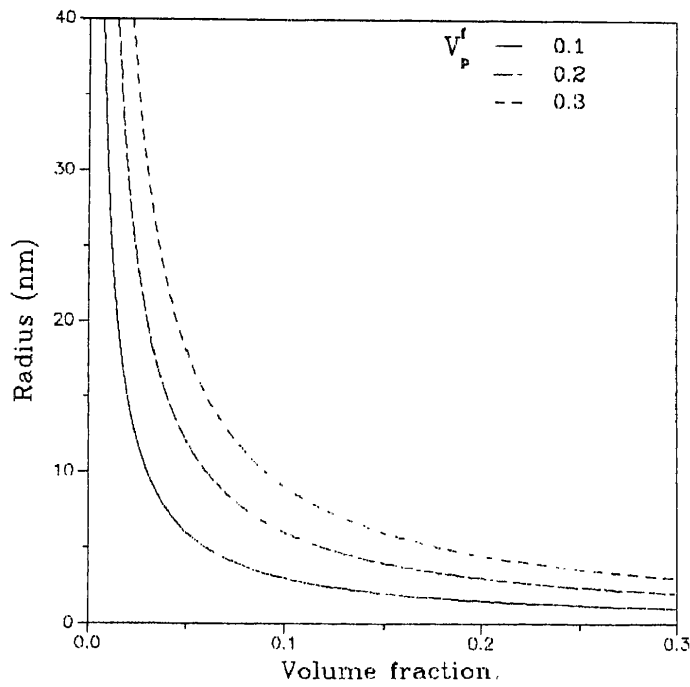


Figure 2. A plot showing the volume fraction of the dispersed phase-matrix boundary as a function of the size of the dispersoid.

3. Processing of nanocrystals through rapid solidification

Most of the nanocrystalline materials produced to date have been synthesized either from vapour state or from solid state. Excellent reviews dealing with cluster aggregation techniques from vapour state (Birringer 1989; Gleiter 1989; Siegel 1991) and mechanical alloying involving solid phases to produce nanomaterials (Johnson 1986) are available. Controlled devitrification also appears to be a promising route for synthesizing nanomaterials (Yoshizawa *et al* 1988). Little efforts are, however, made to probe the efficacy of rapid solidification techniques for producing nanomaterials. We shall now briefly discuss the strategy based on basic solidification principles necessary to successfully produce nanomaterials through solidification routes.

The primary requirements for the production of nanomaterials from liquid are high nucleation rate and low growth rate of the solid phases involved in the liquid–solid phase change. The high nucleation rate can be achieved by increasing the undercooling and kinetically avoiding heterogeneous nucleation. The growth rate, however, also increases with undercooling unless the diffusivity at the growth interface decreases drastically. This is possible in cases where liquid viscosity increases significantly with decreasing interface temperature. Thus proper control of the rapid solidification processing parameters in suitable glass forming systems can in principle produce nanocrystalline materials.

The principles for obtaining nanodispersed two-phase materials or nanocomposites by solidification route are more complex. The process consists of two steps. In the first step the dispersed phase should nucleate in the melt with a high nucleation rate and a low growth rate. In the second step, the matrix phase should nucleate and grow at a very high growth velocity enabling the trapping of the dispersed solid phase co-existing in the melt. Both these conditions are achievable in the rapid solidification processing which involves very high undercooling of the melt.

In determining which system will be amenable for production of nanocomposites, features of the phase diagram play an important role. We have successfully produced nanocomposites in alloys showing liquid miscibility gap. The salient features of the monotectic solidification has recently been reviewed (Mazumder *et al* 1991). The compositions most suitable for such processing lies between the monotectic point and critical temperature of liquid phase separation. As shown in figure 3 the miscibility gap is characterized by two regions, (A) the nucleation and growth regime and (B) the spinodal regime. The effect of rapid solidification by quenching through the latter region is not clear and is a subject of future study. Most of the nanocomposites produced by us have alloy compositions such that on cooling they pass through stable or metastable extension of region A. Although it was believed for a long time that nucleation of phase separating liquid cannot be suppressed, recent work by us and others (Goswami and Chattopadhyay 1992a; Uebber and Ratke 1991) clearly indicate that contrary to the belief, under suitable conditions (including rapid solidification) significant undercooling of the melt is possible before the alloy melt starts phase separating. The undercooling enables a high nucleation rate of the second liquid. We note that the probability of nucleation of matrix phase is, although low, finite. However, the matrix phase once nucleated will grow rapidly because of the fact that the chemical driving force and hence growth rate is directly proportional to the undercooling below the monotectic temperature. The growing matrix interface traps

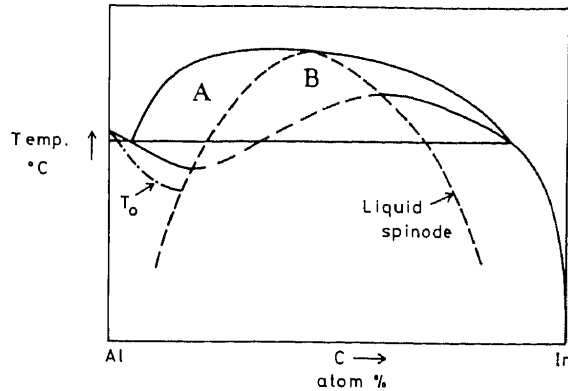


Figure 3. A schematic phase diagram showing liquid state miscibility gap. Separation process in regime A is controlled by nucleation and growth while regime B undergoes spinodal separation.

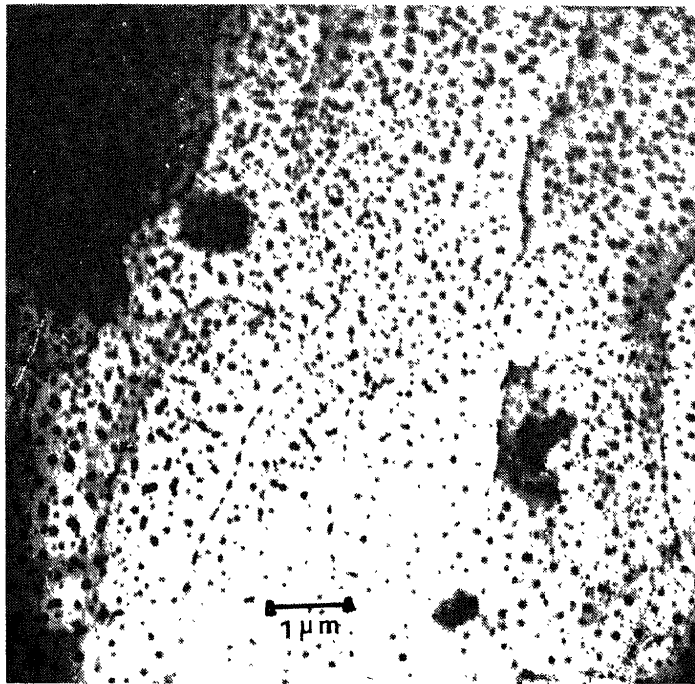


Figure 4. A typical transmission electron micrograph showing the dispersion of nanoscaled Bi particles in aluminium matrix produced by rapid solidification.

the phase separating second liquid. The entrapped liquid phase solidifies later to yield the nanodispersions. Figure 4 shows a typical example of bismuth particles dispersed in aluminium matrix by rapid solidification (Goswami and Chattopadhyay 1992a).

Nanodispersions can also be obtained in the compound forming systems. The essential requirement in that case is a metastable overlap of two-phase fields at an undercooled temperature which is accessible. Additionally the first phase formation should be nucleation dominated. The sequence of formation of nanodispersion is

again similar. The rapid growth of stable phase which nucleates later in the undercooled melt traps the finely dispersed phase formed initially in the liquid to yield a nanodispersed solid. Figure 5 shows the schematics of the possible phase field where such a behaviour is expected. A typical example of $\text{Ti}_2\text{Ni}/\text{TiNi}$ intermetallic nanocomposite is given in figure 6a (Nagarajan and Chattopadhyay 1992).

4. The size limits of the nanodispersed phase

The ultimate size of the nanodispersions depends on the nucleation and growth kinetics of the dispersoids and the trapping conditions. The latter, controlled by the moving interface, also determines the time available for the dispersoids to nucleate and grow. The trapping of second phase by moving interface is a widely studied subject. Different models are currently available to explain the trapping phenomenon (Uhlmann *et al* 1964; Bolling and Cisse 1971; Surappa and Rohatgi 1981; Shangguan *et al* 1992). We shall consider the earliest of these formulations by Uhlmann *et al* (1964) for their underlying simplicity and applicability to the present situation. The basic conditions during the trapping process is illustrated in figure 7. A particle will be pushed ahead of a moving interface due to interfacial free energy dependent repulsive force as long as fluid flows to accommodate particle motion in the space between interface and particle. Beyond a critical velocity, the fluid flow is hindered and particle gets trapped in the matrix. The critical velocity V_c of the moving interface for trapping a particle of size r is given by

$$V_c = 1/2(n+1)(La_0V_0D/kTr^2) \quad (6)$$

where L , the latent heat of fusion of the matrix, V_0 , the atomic volume, D , the liquid diffusivity, a_0 , the atomic diameter of the matrix and T , the interface temperature when trapping is occurring. The constant n has usually a value of 3. This analysis ignores the effect of thermal conductivity of the dispersoids lying ahead on the interface shape and the viscous drag of the suspended particles during pushing. In our case the small size of the particles justifies the neglect of these effects.

Clearly any size of particles r can be trapped provided the interface moves with sufficient velocity. However, as the size of the particles becomes smaller, the velocity

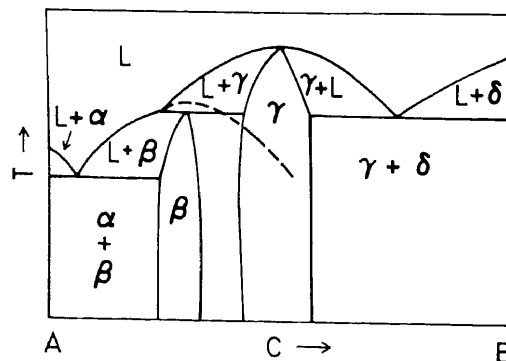


Figure 5. Schematic of a phase diagram showing overlapping phase field when the boundaries (dashed line) are metastably extended. Such systems in the regions are candidates for the production of nanocomposites by rapid solidification route.

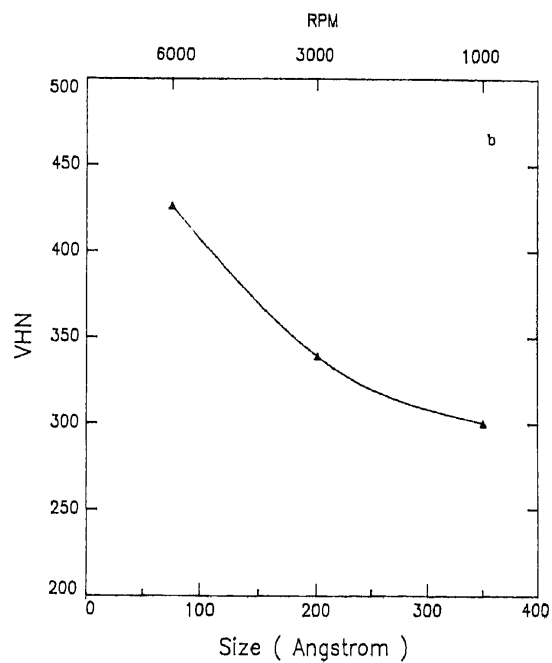
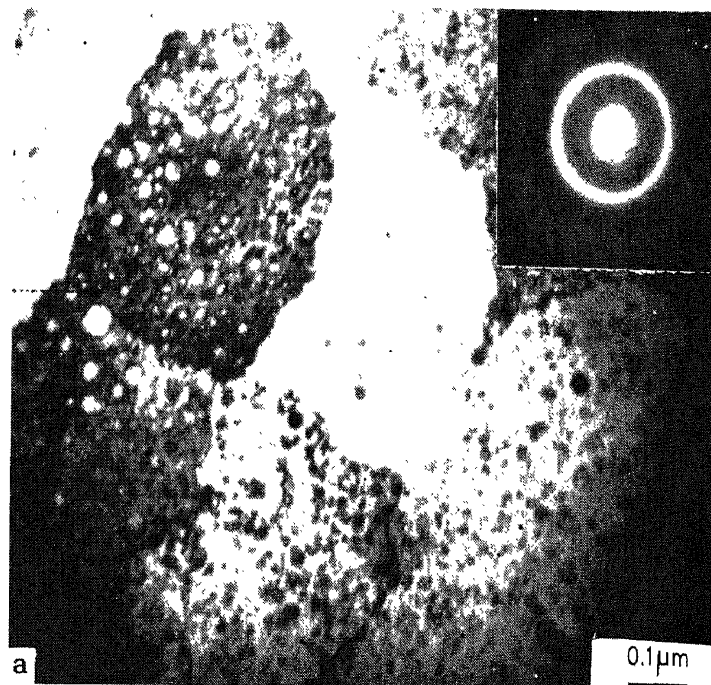


Figure 6. a. A typical bright field transmission electron micrograph of $Ti_2Ni/TiNi$ intermetallic nanocomposites. Inset shows diffraction pattern from the nanoparticles. b. A plot of hardness vs processing wheel speed in $Ti_2Ni/TiNi$ nanocomposites.

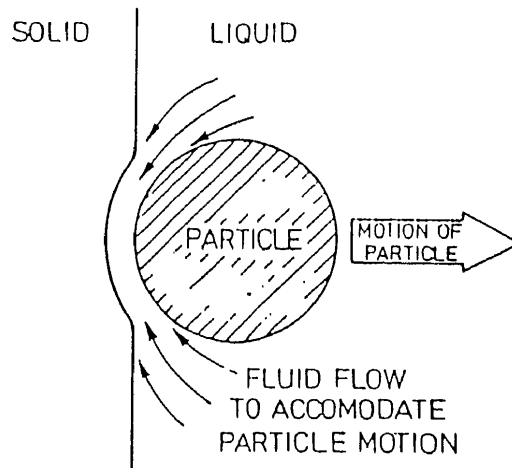


Figure 7. A schematic of the trapping process of the dispersed phase in liquid by a moving interface.

required for trapping increases parabolically. For the production of nanocomposites by the liquid route, the limit of interface velocity of the melt-matrix interface primarily determines the scale of the dispersoids. For monotectic systems involving aluminium and zinc, the constant r^2v is found to be of the order of $10^{-18} \text{ m}^3 \text{ s}^{-1}$. This analysis assumes a planar interface and ignore drag on the interface due to dispersion in the liquid. One can also estimate the limiting size. Assuming the maximum velocity with which a liquid–solid interface can move is of the order of 1 m s^{-1} , the critical size for trapping turns out to be $\sim 3 \text{ nm}$ for zinc alloys. This may represent the limit to the size that liquid route can achieve in the production of nanocomposites.

5. Characterization of nanocomposites produced by liquid–solid transformation route

As discussed earlier, the nanocomposites obtained by rapid solidification can be classified into two classes in terms of the nature of the liquid phase. The liquid phase can either show clustering or compound forming tendencies. In the former the dispersoids are initially in the liquid state while in the latter the solid nanoparticles are trapped by the moving interface. The difference gets reflected in the nature of the second phase microstructure. Although both exhibit fine dispersoids, the dispersoids in systems showing liquid clustering exhibit orientation relations with the matrix. This is due to the fact that the solidification of the entrained liquid droplets is catalysed by the surrounding matrix. The morphology of the dispersed phase in immiscible alloy systems is distinct and can be predicted from the intersection point group of the entrapped liquid and solid matrix (Cahn and Kalonji 1982; Goswami and Chattopadhyay 1992b). In contrast the nanocomposites in intermetallic phase forming systems exhibit a completely random distribution (Figure 6a) (Nagarajan and Chattopadhyay 1992). The selected area diffraction patterns exhibit smooth Debye-Scherrer rings (see inset of figure 6a). The grain boundaries in these cases are not straight due to the pinning action of dispersoids. Analysis of such boundaries are currently under way. Coarsening of nanocomposites at higher temperatures

releases significant interfacial energies which can be followed in differential scanning calorimeter. Such a heat effect is unknown in conventional alloys.

The hardness of the nanocomposites containing hard intermetallic phase is expected to increase significantly. An example is shown in figure 6b. The hardness is found to scale with particle size and in turn with processing parameters like wheel surface velocity. Efforts to study dislocation motions in these materials are at a preliminary stage. In systems containing liquid immiscibility, the dispersoids are soft and low melting. One predominantly observes dislocation cutting through the dispersoids (Singh *et al* 1992). The hardness in general increases with the increasing cooling rate (effected by higher wheel speed in chill block techniques of rapid solidification) and therefore, decreasing particles size. Occasionally a minimum could be observed in certain nanocomposites which are yet to be understood. An example in Zn-Bi system where Bi particles are dispersoids is shown in figure 8.

The nanoscale ultrafine microstructure is expected to alter the properties significantly. We have already shown ultrafine lead dispersions make the surrounding matrix superconducting at temperatures much higher than the matrix superconducting temperature (Goswami *et al* 1992). Figure 9 shows a typical example for Al-Pb nanocomposite. In this case the entire aluminium matrix has become superconducting at 4.5 K while superconducting temperature of aluminium is only 1.198 K. The magnetic and electrical properties are also expected to exhibit new properties. Thus a systematic study of properties of these materials is necessary. Efforts in this direction are currently under way.

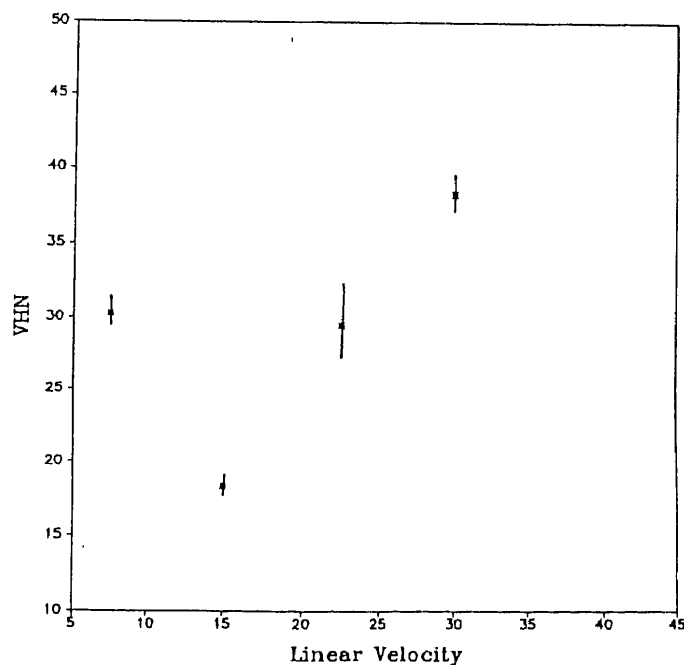


Figure 8. A plot showing hardness as a function of processing parameter (linear velocity of wheel) in Zn-10wt% Bi alloy. The latter scales with particle size. Note the minimum in hardness.

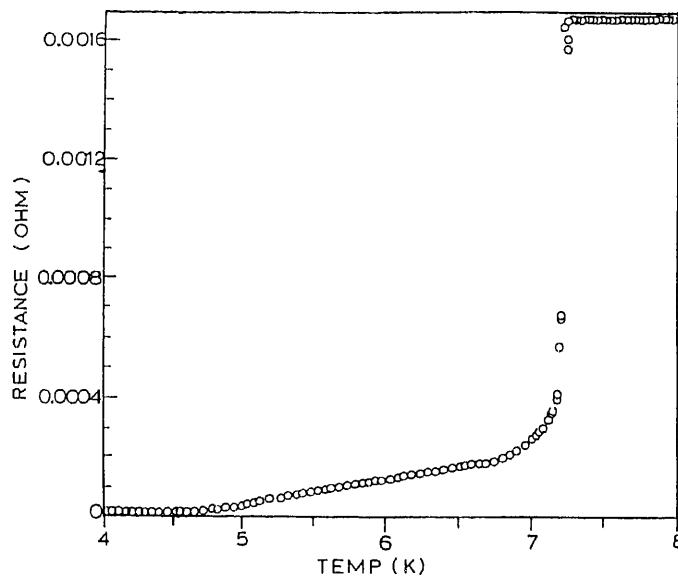


Figure 9. The resistivity of an Al-15wt% Pb nanocomposite showing enhancement of matrix superconducting transition.

6. Conclusions

It is shown that an increase in boundary component in a given volume can be obtained by reducing the grain size. For nanocomposites containing nanoscale dispersoids, it is possible to have large boundary components although the matrix grain can be much coarser. It is also possible to produce nanocomposites from liquid state through rapid solidification by a nucleation dominated formation of the dispersed phase from melt and their subsequent trapping by the moving interface. The conditions for trapping and limits of scale of dispersion can be predicted by using the theory of particle trapping by Uhlmann *et al* (1964). Nanocomposites can be produced in systems showing miscibility gap as well as in systems showing affinity for compound formation. In the former case a distinct orientation relation between the matrix and dispersoids could be observed. Such an orientation relation is absent in the latter case. The preliminary study of the properties including hardness and electrical resistivities suggests interesting variations which need to be investigated.

Acknowledgement

It is with a deep sense of gratitude the author acknowledges the sustained encouragement, and support from Professors T R Anantharaman, P Ramachandrarao, S Lele and S Ranganathan in chartering new course and the enthusiasm and creativity of his students, R Goswami, R Nagarajan, B Mazumdar and S B Singh who have made this study possible. The fruitful collaborations with Dr B Cantor, Dr K Aoki and Prof. A K Roychaudhury are gratefully acknowledged.

References

- Birringer R 1989 *Mater. Sci. Engg.* **A117** 33
Bolling G F and Cisse J A 1971 *J. Cryst. Growth* **10** 56 1981
Cahn J K and Kalonji G 1982 in *Solid-solid phase transformation*, (eds) H I Aaronson, D E Laughlin, R F Sekerka and C M Wayman (Warrendale, USA: AIME) p. 3
Gleiter H 1989 *Prog. Mater. Sci.* **33** 223
Goswami R and Chattopadhyay K 1992a (unpublished work)
Goswami R and Chattopadhyay K 1992b *Nanostruct. Mater.* (communicated)
Goswami R, Banerjee S, Chattopadhyay K and Roychoudhury A K 1992 *J. Appl. Phys.* (communicated)
Jena P, Rao B K and Khanna S N (eds) 1989 *Physics and chemistry of small clusters*, (New York: Plenum Press)
Johnson W 1986 *Prog. Mater. Sci.* **30** 81
Mazumder B, Goswami R and Chattopadhyay K 1991 *Metals, Materials & Processes* **2** 293
Mütschele T and Kirchheim 1987 *Scr. Metall.* **21** 1101
Nagarajan R and Chattopadhyay K 1992 *Acta Metall. Mater.* (communicated)
Shangguan D, Ahuja S and Stefanescu D M 1992 *Metall. Trans.* **A23** 669
Siegel R W 1991 *Ann. Rev. Mater. Sci.* **21** 559
Singh S B, Goswami R and Chattopadhyay K 1992 *Scr. Metall. Mater.* (communicated)
Surappa M K and Rohatgi P K 1981 *J. Mater. Sci.* **16** 562
Uebber N and Ratke L 1991 *Scr. Metall. Mater.* **25** 1133
Uhlmann D R, Chalmers B and Jackson K A 1964 *J. Appl. Phys.* **35** 2986
Yoshizawa Y, Yamayuchi K and Ogama S 1988 European Patent 0271 657-A2, 22.06